Fluoride Capture Capacity of SGA: The Interplay Between Particle and Pore Size Distributions

Gordon E.K. Agbenyegah, Grant J. McIntosh, Margaret M. Hyland, and James B. Metson

Abstract

The Bayer process, storage and transport of smelter grade alumina (SGA) together contribute to the unique particle size distribution of the SGA as received in a gas treatment facility or in a reduction cell hopper. Pore size distribution analyses of alumina fractions indicate that the +125, +90 to −125, +63 to −90 and +45 to −63 μm particles possess similar total pore volumes. The total pore volume of −45 μm particle size fraction, however, was found to be approximately 15% lower than the remaining bulk. Having earlier studied the evolution of pore size distribution in the bulk SGA during fluoride scrubbing, this work examines the interplay between particle and pore size distributions, with focus on the impact of fines on scrubbing efficiency in a smelter GTC.

Keywords

Particle size distribution • Pore size distribution • Alumina • HF • Gas treatment

Introduction

The main feedstock for primary aluminum production is smelter grade alumina (SGA or alumina) but it also utilized as the primary adsorbent in a smelter gas treatment centre (GTC) for the capture and return of particulate and gaseous fluorides. Considering, the dual role of alumina, its quality must meet the standards required for optimum operations of the potroom and the GTC. Generally, the SGA quality parameters reported on specification sheet include gibbsite and alpha alumina content, particle size distribution, attrition index, loose bulk density, BET surface area, loss on ignition, sodium oxide content, silicon oxide and the concentration of other impurities. The quality of alumina is vital to a smelter's endeavor to meet production targets, metal purity, energy efficiency and environmental benchmarks.

Smelters fitted with GTCs specify alumina with optimum surface area for maximized capture of fluoride fumes. However, without pore size distribution data on the specification sheet, the BET surface area alone is misleading and insufficient for predicting alumina performance in a GTC. The importance of the presence of accessible pores has been highlighted by earlier researchers [1] who unanimously assert that the smallest pores may pose kinetic limitations during dry scrubbing. McIntosh et al. [2] have demonstrated, by modeling the evolution of the pore size distribution of industrial and laboratory fluorinated aluminas, that pore blocking and inhibition due to surface-diffusion are responsible for the depletion of reactive sites. The authors also posit that pores less than 3.5 nm are ineffective towards removing fluorides from potroom exhaust gas streams and advocate that a BJH surface area for pores >3.5 nm should be reported on alumina specification sheets instead of an averaged BET specific surface area.

G.E.K. Agbenyegah · M.M. Hyland
Department of Chemical and Material Engineering, University of Auckland, Private Bag 92019, Auckland, 1142, New Zealand

G.E.K. Agbenyegah (✉) · G.J. McIntosh · M.H. Hyland J.B. Metson
Light Metal Research Center, University of Auckland, Auckland, New Zealand
e-mail: proffzee@yahoo.com

G.J. McIntosh · J.B. Metson
School of Chemical Sciences, University of Auckland, Auckland, New Zealand

© The Minerals, Metals & Materials Society 2017
A.P. Ratvik (ed.), *Light Metals 2017*, The Minerals, Metals & Materials Series,
DOI 10.1007/978-3-319-51541-0_60

The precipitation stage of the Bayer process (by which SGA is produced) heavily influences the particle size distribution, whereas the calcination stage impacts the alumina phase distribution and pore size distribution. During precipitation, the seeding, agglomeration and grain growth steps determine the particle size distribution of the gibbsite precursor prior to calcination. However, it is also reported [3] that depending on calcination technology, particle breakage and attrition can produce the differences in fines content observed between the starting gibbsite and the final SGA. Fines are defined in the industry as particles <45 μm in diameter. The residence time of the various gibbsite particles and the heating rates during calcination yield a heterogeneous mix of agglomerates with phases ranging from gibbsite to alpha alumina and a pore size distribution spanning nano- to macro-porosity. Although HF capture and its effect on the pore size distribution has been discussed [2, 4], the evolution of pore size distribution for specific particle size ranges have not been studied in-depth.

Coyne et al. [5] studied the influence of particle size distribution on HF adsorption capacity on SGAs from different Bayer plants (three by flash calcination and one by kiln calcination). The samples were sieved into +150, +125 to −150, +106 to −125, +75 to −106, +45 to −75 and +20 to −45 μm fractions. The samples were reacted with 155 mg/Nm^3 HF in a fixed bed reactor at 120 °C for a one-hour period and subsequently characterized for BET surface area, alumina phases (γ, Δ, θ, χ, α), surface acidity, MOI (moisture on ignition), LOI (loss on ignition) and residual soda content (Fig. 1).

Irrespective of calcination method, the 106 to −125 μm fraction showed a maximum fluoride adsorption. The authors found that only the MOI content of the various particle size fractions followed a similar trend as fluoride adsorption and showed a maximum F adsorption for the 106 to −125 μm fraction. Coyne et al., however, could not explain why water easily removed by heating SGA to 300 °C i.e. MOI (25–300 °C) is highest in a particular particle size fraction and its apparent correlation with the amount of HF adsorbed. Interestingly, the fines (−45 to +20 μm) consistently captured the least amount of F per unit surface area.

Increased content of fines in SGA is known to be responsible for a myriad of challenges in a smelter, including dusting [6], reducing air-slide system capacity [7], anode cover/crust collapse [8], alumina dosage, dissolution problems and increased anode effect frequency [9]. The inclusion of under-calcined (gibbsitic) electrostatic precipitator (ESP) dust in the final SGA product has been observed to correlate with a bi-modal pore size distribution, high BET surface area and increased HF generation [1]. Some calciners, by design and operation, may generate over-calcined ESP dust which is expected to lower the BET surface area of the bulk SGA upon inclusion.

With segregation and attrition taking place as primary alumina is transported from port to pot, the impact of fines

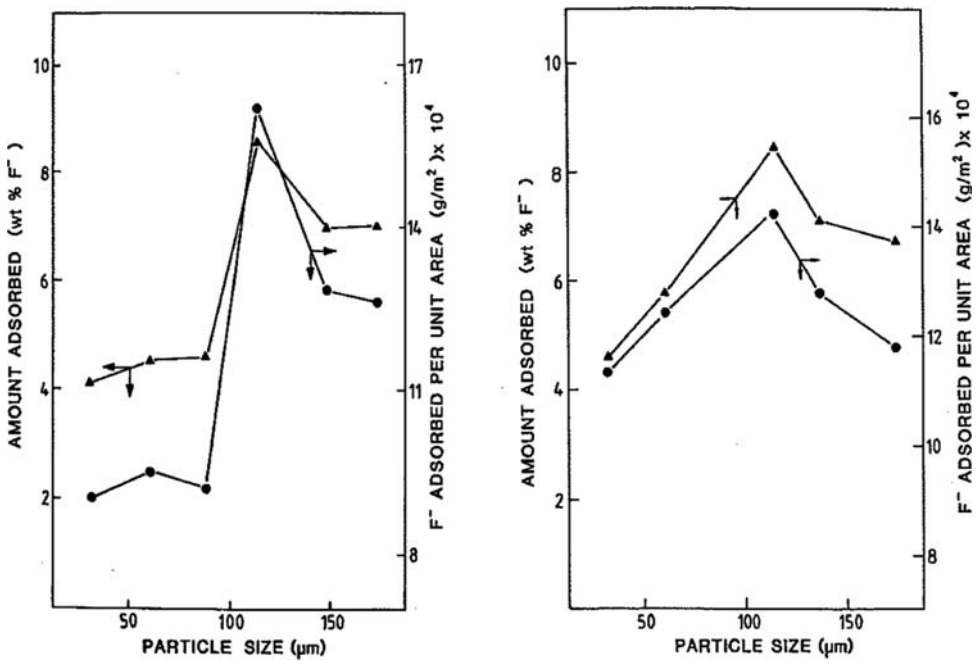

Fig. 1 Fluoride adsorption versus mean particle size for flash calcined SGA (*left*) and kiln calcined SGA (*right*) [5]

on the performance of the dry scrubber also needs to be reassessed.

Experimental Method

Breakthrough experiments for this study were carried out in a lab scale scrubber. The reactor is a cylindrical stainless steel column (16.5 cm height × 1.5 cm diameter) with an HF-resistant fluoropolymer coating. Sieved fractions of smelter grade alumina were reacted with dry HF gas at a temperature of 100 °C. The fractions are as follows:

- −45 μm
- +45 to −63 μm
- +63 to −90 μm
- +90 to −125 μm
- +125 μm

One gram (1 g) of sieved Al_2O_3 fraction was reacted with 320 mg/Nm^3 (∼400 ppm) of HF until the breakthrough point is attained, where the supply rate of the anhydrous HF exceeds the rate of reaction up to ∼10 ppm. An excellent signal-to-noise ratio is achieved at 10 ppm, hence the specification of the number as the breakthrough concentration. HF concentration was continuously monitored by a Boreal Laser™ tunable diode laser (TDL) in a Teflon-coated gas cell. The path length of the gas cell is 20 cm. Reaction temperature was 100 °C. A starting sample of alumina with particle size ranging from +45 microns to −125 microns with 0.03% of −45 μm particles was utilized in a second set of experiments. Incrementally, 10, 20, 30 and 40% of fines (−45 μm grains) were added to the starting Al_2O_3 material. The experiments were carried out with 320 mg/Nm^3 HF. All reactions were maintained at 100 °C.

Characterization

The fluorinated aluminas were characterized for surface area and pore size distribution by N_2 adsorption with a Micromeritics Tristar 3000 equipment. The isotherm data was subsequently utilized for constructing the pore size distribution and modeling of the pore size evolution with fluorination. Particle size fractions were confirmed after mechanical sieving with a Malvern Mastersizer 2000 equipment. Phase identification and X-ray patterns of the alumina fractions were obtained with a Panalytical™ Empyrean diffractometer. A KRATOS® Axis Ultra X-ray photoelectron spectrometer (XPS) equipment was employed for collecting chemical state information about the reaction product formed on the alumina surface.

Results and Discussion

XRD patterns of SGA fractions in Fig. 2 indicate that alpha content increased as particle size decreased.

Results published by earlier investigators [9] exhibit a similar trend. Breakthrough curves (reactor exit concentration versus time) for the reactions of HF with the particle size fractions are shown in Fig. 3.

It is evident from the breakthrough plots that the sub 45 μm particles captured the least amount of fluoride before reaching breakthrough point. Generally, the particles >63 μm perform to about the same extent in terms of F captured. The table below shows the BET specific surface area (SSA), cumulative pore volumes and the amounts of

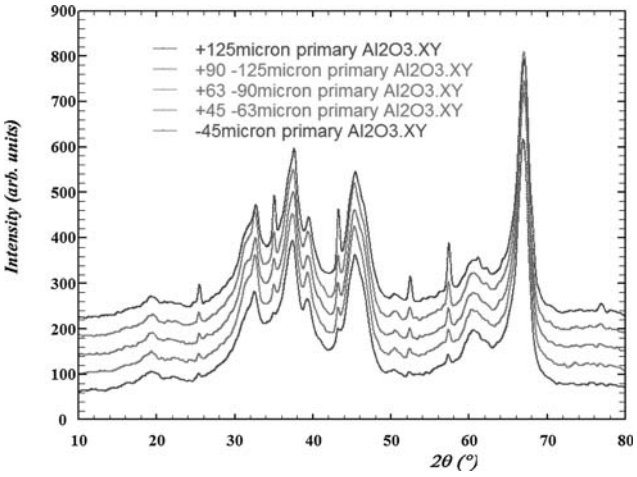

Fig. 2 XRD scan of sieved alumina particle fractions

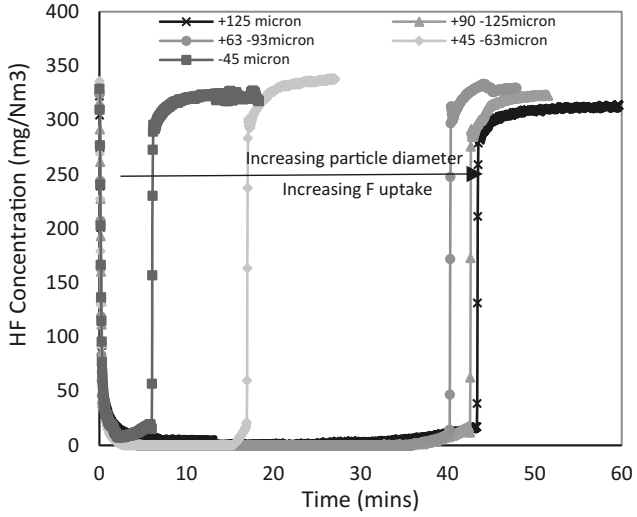

Fig. 3 Breakthrough curves for reaction of HF gas with various alumina fractions

Table 1 Results of surface property changes with HF reaction

SGA fractions (μm)	Cumulative pore vol. (cm^3/g nm)	Primary BET SSA (m^2/g)	Fluorinated BET SSA (m^2/g)	F captured (wt%)
−45	0.17	58	48	0.1
+45 to −63	0.18	63	62	0.2
+63 to −90	0.20	65	64	0.6
+90 to −125	0.20	67	65	0.7
+125	0.20	70	68	0.7

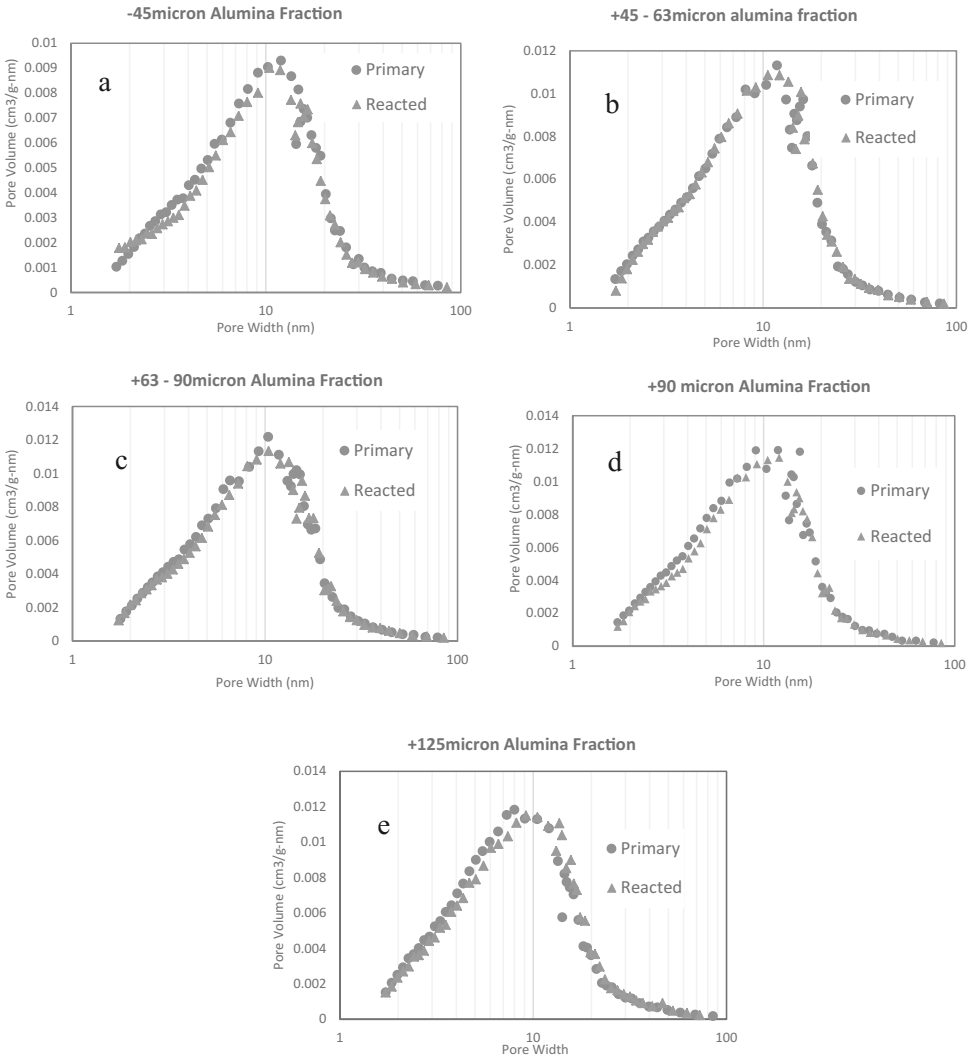

Fig. 4 **a–e** Pore size distribution of SGA fractions, primary and reacted (fluorinated)

fluoride scrubbed at breakthrough for the individual particle fractions.

It is noteworthy that the BET SSA and cumulative pore volume of sub 45 μm particles was the least when compared with the remaining fractions (Table 1). An equally instructive observation is the significant reduction in BET SSA of the fluorinated sub 45 μm fraction although it underwent the least exposure to HF gas. The reason for the low HF capture by the fines will be better explained with results of breakthrough experiments, where fines are increasingly added to the primary SGA. The following diagrams (Fig. 4 a–e) show the pore size distribution of the different SGA fractions (primary and fluorinated).

The −45 μm particles have ∼15% less total pore volume than the remaining fractions investigated (Fig. 5) which is one of the probable reasons for the poor performance of the fraction. It is also noteworthy that the fines fraction are likely to include over-calcined super-fines (particles less than

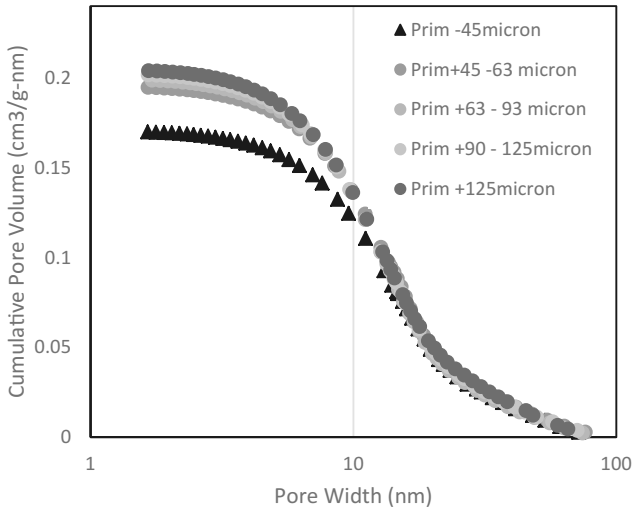

Fig. 5 Cumulative pore volumes of primary SGA fractions

20 μm) which were neither quantified nor analyzed for the purposes of this study.

Incremental Fines Addition

The presence of excessive fines in the primary SGA injected in GTC reactors and its ramifications for fluoride scrubbing efficiency is sparsely documented. Smelters have managed segregation and attrition by transporting alumina from the port to silos by angled air-slides and by trucks. Anti-segregation systems have been developed to mitigate the impact of silo filling and emptying on the accumulation of fines. For injection type scrubbers, fines in the primary adsorbent SGA may change the dynamics of the alumina-HF reaction. Chandrashekar et al. [10] published data collected from a smelter that showed that increase in fines content of alumina directly resulted in increased emission of particulate and gaseous fluorides.

As earlier-mentioned, fines in SGA may be under-calcined gibbsite which would increase hydroxyl content resulting in increased continuous HF generation [11]. Gibbsitic fines possess not easily-accessible porosity, thereby making it more challenging when the same SGA with an over-estimated BET SA is also utilized in the GTC as scrubbing material. When SGA fines are predominantly over-calcined alpha phase alumina, a low BET SA constraint tends to limit the amount of fluoride that can be captured with respect to the GTC kinetics. Notwithstanding the predominant alumina phases (gibbsite or alpha) present in SGA fines, powder fluidization issues such as minimum fluidization velocity, flowability, dense phase voidage and pressure drop issues still pertain and could impact the scrubbing efficiency.

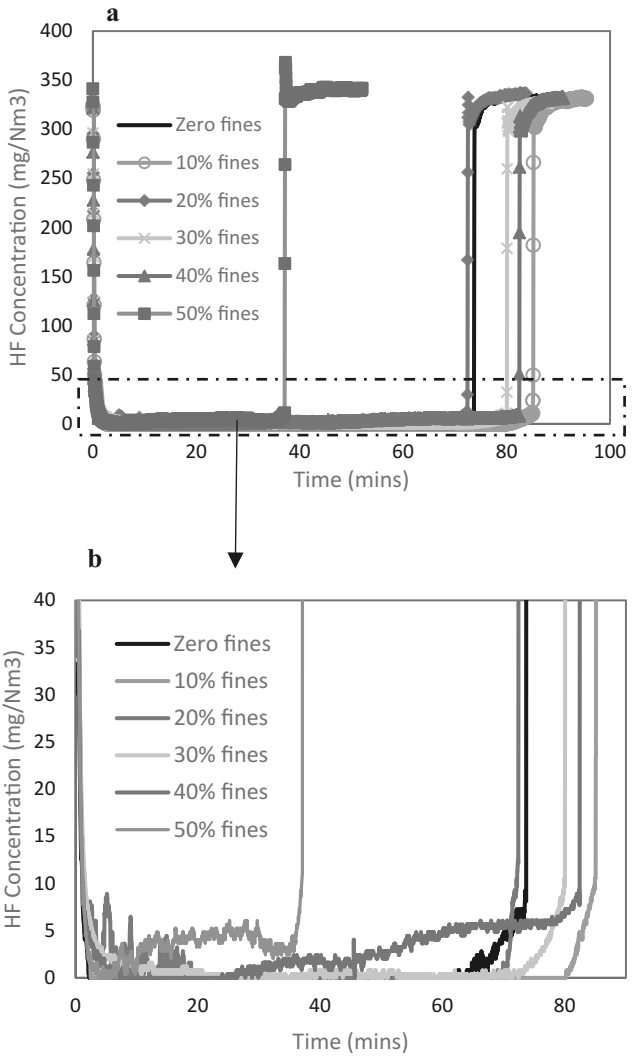

Fig. 6 **a** Breakthrough curves for HF reaction with SGA of varying fines content. **b** Breakthrough curves showing the early inception of breakthrough for high fines samples

In order to ascertain the influence of fines in the bulk SGA injected into the GTC reactor, breakthrough experiments were performed with increasing levels of fines in the adsorbent SGA. Breakthrough curves for the reactions are shown in Fig. 6a, b (inlet [HF] = 320 mg/Nm^3, T = 100 °C).

A glass column of similar dimensions as the Teflon-coated steel reactor was used to observe the fluidization patterns/regimes of the increasing fines samples. Bed heights and minimum fluidization velocities were also measured. N_2 gas at 25 °C was the fluidizing gas.

Some effects of increased fines in the adsorbent alumina are immediately obvious from the breakthrough curves (Fig. 6). With the exception of the 10 and 20% fines sample, it is seen that reactor exit HF concentration does not stabilize at zero during the reaction with the 30, 40 and 50% fines samples. As fines content increases, exit HF concentration

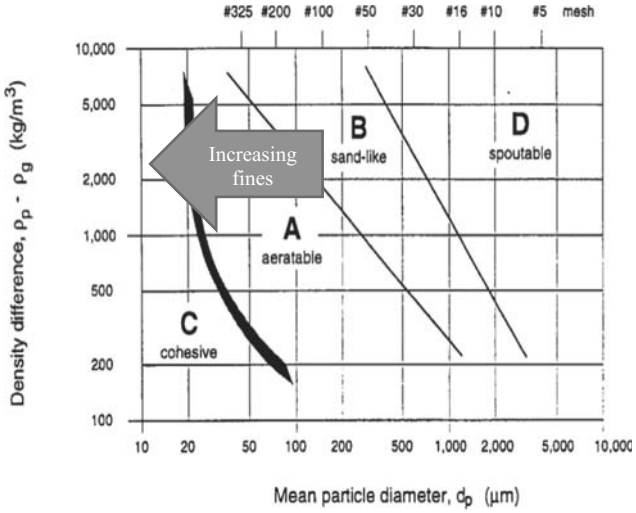

Fig. 7 Geldart chart [13]. The superimposed *arrow* shows changing powder characteristics with increasing SGA fines content

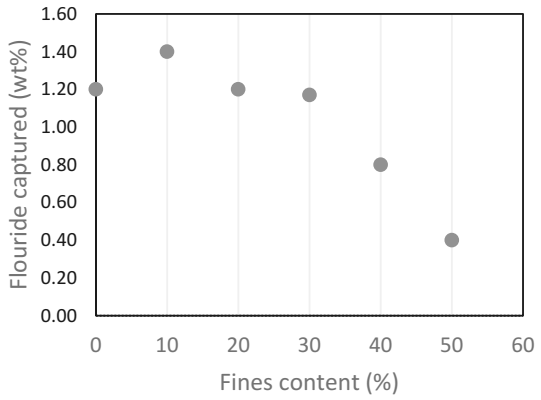

Fig. 8 Fluoride loadings of SGA with varying fines content

reaches a value greater than zero significantly earlier and steadily rises to attain the breakthrough value.

The 10% fines content sample performed better than the zero fines sample even for repeat runs. It is likely that the increase in particle number presents more reaction surface area, hence the better performance translating to longer breakthrough times. It is also suggested by Zenz and Othmer [12] that fines acts as lubricants or miniature roller bearings that assist the shear of coarser particles thereby lowering the effective dense phase velocity.

Figure 7 shows the direction which increasing fines in SGA would follow on a Geldart chart [13]. It was observed during the fluidization experiment that the increase in fines content progressively causes the alumina to change in flow character from sand-like to cohesive. As the alumina becomes more cohesive, increased inter-particle forces reduce fluidization performance [14], resulting in the entire bed being lifted as a bed or channels being created for exiting unreacted HF gas. In a smelter, a similar situation may be present when large quantities of SGA fines are introduced into the GTC reactor to scrub the HF-laden pot exhaust gases.

Occasionally, hikes in the fines content of primary SGA are recorded as a result of attrition during transport and handling or as a result of silo inventory management practices. This is likely to have the consequence of intermittent increases in GTC stack emissions. The fluoride loading estimated from the fines addition work show that up to ~65% of the scrubbing capacity can be lost as a result of the presence of 50% fines in the bulk SGA (Fig. 8).

Interplay Between Pore Size and Particle Size Distribution of SGA

XRD analyses of the particle size fractions showed that three alumina phases were consistently present in varying percentages, namely—gamma, theta and alpha alumina (corundum). The breakthrough curves and the pore size distribution measurements showed that the fines had the greatest impact on the scrubbing capacity of the SGA, with increasing fines lowering scrubbing capacity.

The mechanisms by which fines are generated differ from refinery to refinery depending on the precipitation and calcination technologies. Within smelters, attrition and segregation during transport, handling and storage are the common mechanisms for fines generation. The fines used for this study contained mostly alpha alumina which have been earlier characterized [15] and shown to possess larger average pore width, lower total pore volume and lower BET SA than the remaining fractions that were studied. From Fig. 5, the lower cumulative pore volume of the fines in the pore width between 1 and 10 nm lends credence to the XRD results (Fig. 2) that the bulk of the fines are over-calcined alumina. The pore size distribution plot in Fig. 8 also shows the marginal reduction in pore volume as fines are increasingly added (Fig. 9).

Although the pore size distribution of +45 to −63 μm fractions was comparable to the fractions of larger particle size, the amount of fluoride captured was as low as the amount captured with the sub −45 μm (Table 1). This observation cannot be explained with the available results. Additional characterization, particularly MOI/LOI and acid/base sites concentration of the fraction, would be beneficial for understanding the cause of the low fluoride capture at breakthrough. It is expected that fines generated by

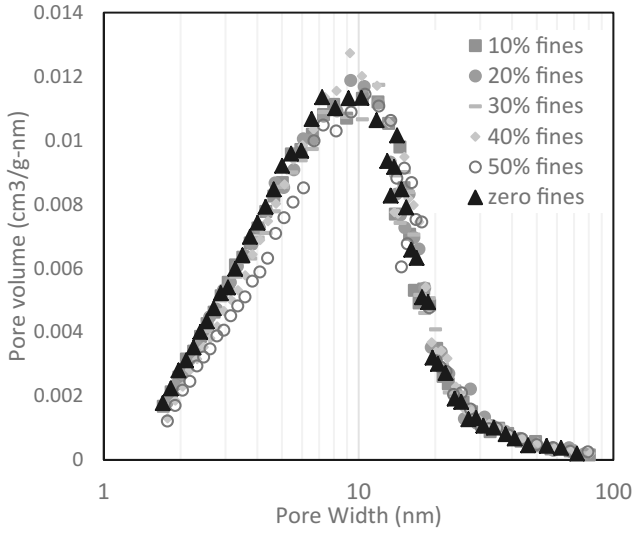

Fig. 9 Pore size distribution of primary SGA of varying fines content

particle breakage during post-refinery transport and handling would maintain the pore size distribution and surface chemistry of the parent particles. In this respect, it is likely that the +45 to −63 μm particles may undergo attrition and also contribute also to poor scrubbing performance of the fines fraction.

Particle size fractions greater than 63 μm generally exhibited same levels of HF scrubbing capacity. This is traceable to the similarity in pore size distribution and total pore volume. Generally, pore size distribution of SGA calcined with the same technology is expected to have similar pore size distribution unless blending with ESP dust, for example, is a process consideration towards reducing dust inventory.

Conclusion

A study of the pore size distribution of −45, +45 to −63, +63 to −90, +90 to −125 and +125 μm fractions of SGA has been carried. The pore size distribution were not different for the fractions in terms of the width and mode of the distribution except for the −45 μm which exhibited low pore volumes for the 1–10 nm pore size range. The fractions predominantly consisted of alpha, gamma and theta phase alumina. After reacting the SGA fractions with dry gaseous HF, the fines were seen to perform the poorest in terms of scrubbing capacity.

The results of an incremental fines addition test demonstrated that the presence of excessive fines in SGA, modified it into a cohesive material that is not easily fluidized, thereby decreasing its effective contact with HF gas for optimal scrubbing performance.

Fines are generally undesirable throughout a smelter due to the attendant challenges with transport, dusting, dosage and dissolution in bath. The outcome of this study makes yet another argument for the minimization of the fines content of SGA.

Acknowledgements The authors are grateful to Hydro Aluminum AS for permitting the use of data from a related project for this publication. We also wish to thank Dr. Are Dyroy for his invaluable guidance in writing this paper.

References

1. L.M. Perander, M.A. Stam, M.M. Hyland, J.B. Metson, Towards redefining the alumina specifications sheet—the case of HF emissions, in *Light Metals* (2011), pp. 285–290
2. G.J. McIntosh, G.E.K. Agbenyegah, M.M. Hyland, J.B. Metson, Adsorptive capacity and evolution of the pore structure of alumina on reaction with gaseous hydrogen fluoride. Langmuir **31**(19), 5387–5397 (2015)
3. A. Saatci, H. Schmidt, W. Stockhausen, M. Ströder, P. Sturm, Attrition behaviour of laboratory calcined alumina from various hydrates and its influence on SG alumina quality and calcination design, in *TMS Light Metals* (2004), pp. 81–86
4. G.E.K. Agbenyegah, G.J. McIntosh, M.M. Hyland, J.B. Metson, Assessing the role of SGA porosity in the HF scrubbing mechanism, in *TMS Light Metals* (2016), pp. 521–525
5. J.F. Coyne, M.S. Wainwright, M.P. Brungs, The influence of physical and chemical properties of alumina on hydrogen fluoride adsorption, in *TMS Light Metals* (1987), pp. 35–39
6. D. Wong, N. Tjahyono, M. Hyland, The nature of particles and fines in potroom dust, in *Light Metals* (2014), pp. 553–558
7. M. Karlsen, A. Dyroy, B. Nagell, G.G. Enstad, P. Hilgraf, New aerated distribution (ADS) and anti segregation (ASS) systems for alumina. Essent. Readings Light Met. **2**(6882), 590–595 (2013)
8. H. Wijayaratne, M. Hyland, M. Taylor, A. Grama, T. Groutso, Effects of composition and granulometry on thermal conductivity of anode cover materials, in *Light Metals* (2011), pp. 399–404
9. L.M. Perander, Z.D. Zujovic, T.F. Kemp, M.E. Smith, J.B. Metson, The nature and impact of fines in smelter grade alumina. J. Met. **61**(11), 33–39 (2009)
10. S. Chandrashekar, D. Jackson, J. Kisler, Alumina fines: journey from cradle to grave, in *Alumina, International Workshop, Quality* (2005), pp. 5–9
11. M.M. Hyland, E.C. Patterson, B.J. Welch, Alumina structural hydroxyl as a constant source of HF, in *TMS Light Metals* (2004), pp. 361–366
12. F.A. Zenz, D.F. Othmer, *Fluidization and Fluid-Particle Systems* (Reinhold, New York, 1960)
13. D. Geldart, Types of gas fluidization. Powder Technol. **7**(5), 285–292 (1973)
14. A.R. Abrahamsen, D. Geldart, Behaviour of gas-fluidized beds of fine powders part I. Homogeneous expansion. Powder Technol. **26** (1), 35–46 (1980)
15. L. Perander, *Evolution of Nano- and Microstructure During the Calcination of Bayer Gibbsite to Produce Alumina* (The University of Auckland, 2010)